International Journal of Mechanical, Industrial and Aerospace Sciences
ISSN: 2517-9950
Vol:13, No:9, 2019

Design of a Telemetry, Tracking, and Command Radio-Frequency Receiver for Small Satellites Based on Commercial Off-The-Shelf Components

A. Lovascio, A. D'Orazio, V. Centonze

***Abstract*—**From several years till now the aerospace industry is developing more and more small satellites for Low-Earth Orbit (LEO) missions. Such satellites have a low cost of making and launching since they have a size and weight smaller than other types of satellites. However, because of size limitations, small satellites need integrated electronic equipment based on digital logic. Moreover, the LEOs require telecommunication modules with high throughput to transmit to earth a big amount of data in a short time. In order to meet such requirements, in this paper we propose a Telemetry, Tracking & Command module optimized through the use of the Commercial Off-The-Shelf components. The proposed approach exploits the major flexibility offered by these components in reducing costs and optimizing the performance. The method has been applied in detail for the design of the front-end receiver, which has a low noise figure (1.5 dB) and DC power consumption (smaller than 2 W). Such a performance is particularly attractive since it allows fulfilling the energy budget stringent constraints that are typical for LEO small platforms.

***Keywords*—**COTS, small satellites, sub-sampling, TT&C.

I. Introduction

THE so-called COTS (Commercial Off-The-Shelf) components are now a widespread reality in the aerospace industry. The term is related both to parts, such as electronic components, equipment, test facilities, entire Ground Stations (GSs) and so on, and to a real design methodology, such as an electrical ground support equipment for COTS Radio-Frequency (RF) systems [1]. Both points of view are, definitely, equivalent: choosing a COTS-based design approach means making use of COTS components at each design level. Moreover, the methodology clarifies and defines the techniques which help to perform better the selection of components as a function of certain requirements.

The design requirements of the small satellites that make use of COTS components are mostly environmental, i.e. they depend on the orbit parameters. The space environment is extremely hostile for electronic components since it is affected by strong temperature ranges and radiation. However, in particular conditions, it is possible to find an environment less severe within which the component, even if not space-qualified, could be "survivor" through the adoption of proper strategies of risk mitigation. The use of COTS components has certainly the great benefit to reduce widely the costs of the final product since additional screening and reliability tests/inspections are not mandatorily required. Therefore, in the last years, they have generated a great deal of interest in space research and industry of small satellites, especially for the LEO.

The LEO small satellites are platforms typically designed to orbit at altitude lower than 1000 km, thus in environmental conditions that allow the use of the COTS components. Since they typically have a weight smaller than the geostationary satellites, the small satellites have the benefit of low launch costs, allowing to develop applications based on satellite constellations. However, having a small size, they need integrated electronic equipment that implements a low power consumption digital logic. Even the Telemetry, Tracking & Command (TT&C) subsystem, considered vital for the satellite life, has been reconceived in the last years by adapting to new trends of the market. The TT&C subsystem has to satisfy three main categories of requirements:

- Mechanicals: It has to be small, compact and low weight so that it is compliant to the standard of small satellites;
- Reliability: TT&C requirements have to be guaranteed for all mission years in the worst-case conditions;
- Functional: It has to be able to establish a reliable communication channel at high throughput so that it can transmit data to GS within the short time of visibility due to LEO orbits.

The COTS components are an efficient solution in order to fulfill all these requirements. In literature, analyses regarding the use of these components in the TT&C design have been reported [2], [3], but often these studies are missing of a theoretical approach that relates the system design to the selection of COTS components.

In this paper, we report an innovative procedure for the design of a TT&C subsystem for LEO small satellites fully based on COTS. The procedure adds to the design theoretical approach the guidelines commonly adopted for the selection of the COTS components, which has allowed to improve the system reliability widely. Particular attention has been given to the design of the analog receiver being, in general, more critical. Its design has been entirely based on the Analog-to-Digital Converter (ADC) performance and on adopting the subsampling technique. We have shown that ADC specifications and the subsampling technique have a direct

Funding FSE-FESR.

A. Lovascio, A. D'Orazio are with Dipartimento di Ingegneria Elettrica e dell'Informazione (DEI), Politecnico di Bari, Bari, Italy (e-mail: antonio.lovascio@poliba.it; antonella.dorazio@poliba.it).

V. Centonze is with Space System & Avionic Division, Sitael S.p.A., Mola di Bari, Italy (e-mail: vito.centonze@sitael.com).

impact on the receiver architecture. This result has been, then, used to simplify the architecture as much as possible by making the frequency conversion stage unique. The single stage has allowed decreasing not only the number of components (reducing implicitly the fault probability) but also the DC power consumption, which is much smaller than 2 W. We have also obtained excellent performance in terms of noise figure (1.5 dB).

II. TT&C Description

A. Background

The TT&C module is the main responsible subsystem for the communication with the earth. It is considered as an essential payload of a satellite because without it the satellite monitoring and control would not be possible. TT&C shall transmit the *telemetry* – set of data and information regarding the "health status" of the satellite and all its subsystems – to the GS and shall receive from it the *telecommands* – a set of configuration/update data. Thanks to TT&C the ground operators can monitor the satellite life and act in case of issues/faults. In other words, the TT&C assures the reliability of the satellite, trying to guarantee its functions for all years foreseen by the mission. Other secondary (but not less relevant) features, such as *tracking* and *ranging*, allow better control of the satellite attitude.

The TT&C reliability is strictly related to its functional performance. The TT&C module has to establish a channel communication with the earth and this channel must be effective and reliable. In order to assure the correct transmission and reception of data, the bit error probability must be as low as possible for all conditions which the satellite could be in. The main parameter used to design channel communication is the Bit Error Rate (BER). It is taken into account both in hardware designing and in the Link Budget Analysis (LBA). The BER requirement is usually given in the worst-case, i.e. when the satellite is farther from the earth. For LEOs it occurs just above the horizon. More distance implies more power in order to assure the same error probability, which could be an issue for the small satellites that have typically a limited power budget. BER depends also on bitrate: if it increases, BER could be affected. A higher bitrate is essential to guarantee the complete transmission of the collected data in the few time the satellite is within the GS line-of-sight. This time can be very short (a bit more than 10 minutes at 500 km altitude) for the LEO satellites because of the Third Kepler's Law. For the same amount of data (M) to be transmitted, a shorter visibility time (t_v) requires a higher bitrate (R_S) according to (1):

$$R_S = \frac{M}{t_v} \tag{1}$$

Increasing the bitrate might require more effort in hardware and software designing. For this reason, the TT&Cs are very complex systems that implement on the same hardware analog and digital functionalities, such as in the Software Defined Radios (SDRs). The SDR approach has the great benefit to simplify complex functionalities, such as the modulation of base-band signals, through the programming of a software or a firmware. In the satellite SDR the modulation/demodulation schemes are typically implemented on Field Programmable Gate Arrays (FPGAs), making the hardware less complex, more compact and with lower power absorption due to digital architecture. Only a few functions, such as the filtering, amplification and frequency conversion, are still implemented by analog components. For all these reasons SDRs are becoming more and more common in the TT&C design.

B. LBA

The LBA is a procedure used to design a channel communication in order to guarantee a specific BER requirement with appropriate margins. Even foreseen by European Cooperation for Space Standardization (ECSS) [4], it allows to relate to each other a set of relevant parameters of the communication system both for downlink and uplink. Even the antennas, especially their placement, affect the link budget and can be optimized in order to improve the BER [5]. The LBA is typically performed using (2):

$$\frac{E_b}{N_0} = \frac{P_T L_T G_T G_R}{k T_S R_S} \tag{2}$$

where E_b/N_0 is the Signal-to-Noise Ratio (SNR), P_T is the transmission power, L_T represents the total losses along the channel, G_T and G_R are respectively the antenna gain of the transmitter and the receiver, k is the Boltzmann constant, T_S is the equivalent system noise temperature of the reception system and, finally, R_S is the bitrate on the channel. L_T takes into account all losses, such as losses due to the transmission medium, mismatch losses, polarization losses, etc [6].

Equation (2) is a complete formula that highlights the dependency of bitrate on power transmission (downlink) and indirectly on satellite receiver noise figure (uplink). The formula can be used to analyze both the downlink and uplink communication channel according to which parameter as a function of bitrate is under consideration.

In order to evaluate the TT&C performance, a real scenario has been studied. In this scenario, a small satellite at 500 km altitude has been considered. A 10^{-6} BER requirement has been defined for the space communication channel. The analysis has been performed in the worst-case, i.e. when the satellite is in the point farther from the earth. Just above the horizon, its distance is about 2573 km for the given altitude. Supposing to transmit a Quadrature Phase-Shift Keying (QPSK) signal on an AWGN-type channel, the theoretical E_b/N_0 ratio is about 10.5 dB for such value of BER. In order to simplify the analysis, only space free loss (L_S) has been evaluated being the major contributors in the count of all losses. It has been estimated according to (3):

$$L_S = 10 \log_{10} \left(\frac{c_0}{4\pi f d} \right)^2 \tag{3}$$

where c_0 is the vacuum speed of light, f is carrier frequency and d is the distance between transmitter and receiver, i.e. the

physical length that the signal goes through the transmission medium. If, for instance, a carrier at 2.245 GHz frequency (to be ECSS compliant regarding Space Operation Service) is transmitted, the free-space loss is about -167.7 dB.

To complete the analysis, we also need to make some assumptions regarding the GS. Companies that offer ground segment services characterize the GSs with the G/T ratio. A typical value for this figure of merit is -12.5 dB/°K that has been assumed for our analysis.

Regarding the downlink channel, (2) has been analyzed from the transmission power point of view in order to define a reasonable power requirement. The analysis result is reported in Fig. 1. Equation (2) has been rearranged expressing the transmission power as a function of bitrate, using all assumptions previously done. Curves have been depicted for several values of satellite antenna gain.

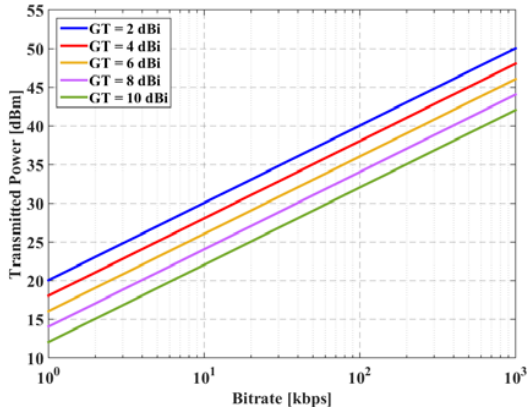

Fig. 1 Transmitted power from satellite versus bitrate for different value of satellite antenna gain

Fig. 1 shows that more than 40 dBm transmitted power with 10 dBi of satellite antenna gain is needed to guarantee 10^{-6} BER at 1 Mbps bitrate. The evaluated power can be decreased by using a reliable communication protocol that foresees, for example, the use of convolutional coding. A robust protocol can protect transmitted data from noise sources and other impairments along the communication channel so that the E_b/N_0 ratio decreases and, consequently, we can save some dBm of power.

Regarding the uplink channel, (2) can be used to estimate the receiver specifications, especially from the noise point of view. A good receiver shall be able to catch and demodulate very weak signals in presence of noise. A figure of merit typically used to characterize the receiver noise performance is the *noise figure* (or *noise factor*). However, since there are several noise sources that affect the signal (galactic, sun and made-man noise), the noise figure is not a good parameter being calculated only taking into account the receiver thermal noise. Thus, for LBA is more common to evaluate the G/T ratio by using (4):

$$G/T = \frac{G}{T_{ant}+T_o\left(\frac{1-L_r}{L_r}+\frac{F-1}{L_r}\right)} \quad (4)$$

where G is the antenna gain, T_{ant} is the total equivalent noise temperature that considers all noise sources that "enter" into the receiver together the signal (noise coming from outside), F is the noise factor (noise generated inside), T_o is the room temperature (290 °K is assumed in space designing) and L_r represents all losses along the path between antenna and the TT&C hardware, such as diplexer losses, coaxial cable losses, etc. The whole denominator of (4) is the equivalent system noise temperature, the same parameter at the denominator of (2).

Following the same approach (and the same scenario) used for the downlink channel and assuming negligible T_{ant} and L_r parameters, we have rearranged (2) to express the noise figure in terms of bitrate in order to evaluate the TT&C performance from the receiver noise point of view. Fig. 2 depicts the noise figure of the receiver as a function of the bitrate for different value of satellite antenna gain having fixed the GS Equivalent Isotropic Radiated Power (EIRP) at 66 dBm typical value.

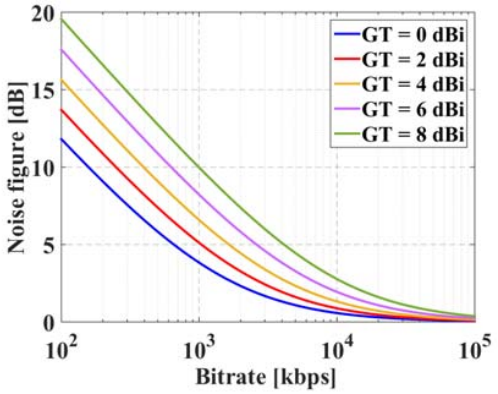

Fig. 2 Receiver noise figure versus bitrate for different value of satellite antenna gain

Fig. 2 shows that for a 1 Mbps bitrate the receiver noise figure is smaller than 5 dB for a 0 dBi satellite antenna gain.

C. In-flight Flexibility

One of the most innovative aspects of TT&C is its flexibility, i.e. the possibility to change the functional parameters without modifying the hardware. Since the modulation algorithms are implemented as firmware on digital components, they can be made adjustable according to the final application using the same board. The firmware configuration is usually decided and implemented at the factory level, but in recent years it is exploring the opportunity of in-flight firmware configuration. This implies that by means of the same telecommand used to control the satellite, ground operators can change the current configuration of the FPGA firmware in order to adapt the TT&C to different needs, such as an orbit change. The same uplink channel could be used to transmit on-board an upgrade of the communication protocol, making the channel even more robust than it was.

The idea is to have a way to adapt the current firmware to the changes of missions, environmental conditions, temporary loss of power, etc. Obviously, not all parameters can be made

adjustable. Typically, bitrate, modulation schemes, code rates can be made adjustable; as well as transmitted power by more effort.

Reducing transmitted power is always a challenge. The power is always a limiting aspect in the space design. Thanks to the possibility to deliver less power in telemetry transmission, better performance in terms of harmonic distortions, spurs, gain compression, etc. are possible. More linear behavior of the power amplifiers is achieved. In recent years, architectures that implement a control system of the power and linearity have been studied. They are the concrete result of benefits offered by the advances in technology, especially in terms of miniaturization of the digital logic and the conversion devices between digital and analog "world".

III. TT&C Receiver Design

A. Requirements and High-Level Architecture

In this section, the design of TT&C with particular emphasis on the analog receiver is discussed both from electrical and mechanical (size and weight) performance point of view. System requirements and a high-level architecture have been defined considering three inputs as starting points:

- The LBA performed in Section II *B*;
- Market research of similar devices;
- The target of applications.

The LBA has allowed defining a reasonable transmitted power and noise figure requirement. Moreover, starting from what the market offers, commercial devices have been analyzed from the technical performance point of view in order to define goals, functionalities and similar requirements (and better in some cases). Finally, the definition of requirements has considered the target of applications, i.e. the small satellites at LEO.

Table I summarizes the set of the high-level and functional requirements of the TT&C.

TABLE I
TT&C Requirements

Requirement	Unit
receiver operation frequency	2025-2110 MHz
transmitter operation frequency	2200-2290 MHz
modulation schemes	QPSK, OOPSK
bitrate in transmission and reception	1 kbps-1Mbps (in-flight variable)
RF transmission power	30-37 dBm (1 dB step variable)
receiver DC power absorption	< 2 W
transmitter DC power absorption	< 15 W
receiver noise figure	< 2 dB
transmitter EVM	< 10%
weight	< 2.5 kg
size	< 140 x 140 x 40 mm
communication protocol with OBC	SpW, CAN
radiation tolerance	< 15 krad
operative temperature	-30°C/+50°C
operative lifetime	5 years

The operation bandwidths of the transmitter and receiver have been chosen to be compliant with the frequency range that ECSS allocates for the Space Operation Service, whose telemetry and tracking functionalities make part [5]. Bitrate and transmitted power requirements have been the result of the LBA while the DC power absorption has been derived by a preliminary power budget analysis.

We have not assigned a specific BER requirement since BER is a specification of the whole satellite system. It is related to the mission parameters, such as orbit, altitude, etc., as the LBA has shown. From the single TT&C module design point of view, it is more useful the performance characterization in terms of noise figure and EVM. For the receiver design, the noise figure was the starting point that has allowed to choose the best architecture and select the most appropriate components in order to guarantee all requirements both of the TT&C and the entire satellite.

Table I shows also mechanical and reliability requirements. Weight and size are derived by a combination of existing commercial modules and the target of applications. Regarding radiation tolerance, the requirement has been defined starting from the target of applications and used in order to make a proper selection of the COTS components. The use of COTS components always implies a certain failure risk in design, but it can be mitigated adopting particularly strategies of hardware implementation and following the suggestions laid down by ECSS [7], [8] as described in detail in Section III *D*. A typical hardware strategy is the redundancy. It has been foreseen for TT&C design, but only for the On-Board Computer (OBC) communication interfaces. Two redundant Space Wire (SpW) interfaces have been assigned for the high-rate data transmission towards/from OBC since it is a robust and reliable protocol. A simple redundant Controller Area Network (CAN) interface has been instead allocated for the control of the unit from the OBC.

Fig. 3 shows the high-level architecture of the entire TT&C module.

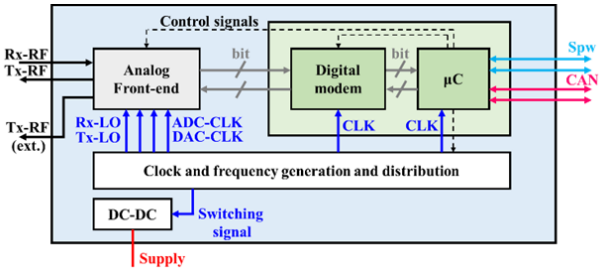

Fig. 3 TT&C high-level architecture with submodules and interfaces

TT&C is constituted by different functional submodules:

- Microcontroller;
- Digital modem;
- Analog front-end;
- A system of clock and frequency generation and distribution;
- A system of power generation and distribution.

The microcontroller is the core of the TT&C. It is in charge of unit control and managing the communication with the OBC formatting the data for the SpW protocol. The

microcontroller receives the commands from OBC by CAN bus in order to adjust bitrate, transmitted power, and other parameters; as well as it acquires the internal telemetry of the module.

Digital modem contains the firmware architecture that processes the modulation and the demodulation of the signals. It implements the modulation schemes, the matching filters, the code system, timing and carrier recovery systems, the equalizer, and other functional components of a typical modem. It operates in base-band at a fixed symbol rate. The bitrate adjusting capability is possible thanks to the system of interpolation and decimation filters, allowing the multi-rate signal processing. In addition, the hardware and firmware have been conceived for a pass-band sampling and exploit the subsampling technique, described in detail in Section III *B*.

The analog front-end is made of a reception and transmission chain, an ADC, a Digital-to-Analog Converter (DAC), a Power Amplifier (PA) and an RF switch. The architecture is shown in Fig. 4. An innovative aspect of this architecture is in the possibility to control the transmitted power through an RF switch. The microcontroller can send a command to RF switch in order to switch on the internal PA or select a path for the signal where there is not a final power amplification. In other words, the switch provides the capability to bypass the internal PA in order to give the user the possibility to add an external one.

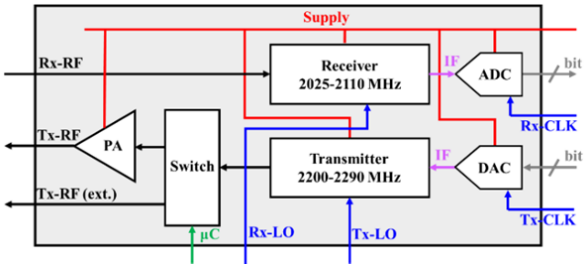

Fig. 4 Functional architecture of TT&C analog front-end

The architecture in Fig. 4 includes also the ADC and DAC although they are not properly analog components. They are conversion devices that work on two different domains (analog and digital) but, anyway, have been considered in the front-end because their detail requirements have driven the design of both receiver and transmitter chains. They have been the first components to be selected starting the noise figure curves analyzed in the LBA (see Fig. 2).

The clock and frequency generation and distribution subsystem generates all frequencies used by TT&C module. It provides two different clock signals for the ADC and DAC and other two different clock signals for the FPGA of digital modem and for the microcontroller.

The core of the subsystem is composed of four Phased-Locked Loop (PLL) and a very stable oscillator. Two PLLs are used for the frequency conversion operations in the transmission and reception chains of the analog front-end. Two other PLLs are used to clock the ADC and DAC. Finally, the oscillator is used to generate the switching frequency of DC-DC converter. As shown in the frequency plan depicted in Fig. 5, the submodule works using a unique stable 40 MHz Temperature Compensated Crystal Oscillator (TCXO) that has ±2.5 ppm frequency stability over TT&C operative temperature (-30 °C/+50 °C). All PLLs receive such a reference signal in order to keep the phase coherence on all submodules. This prevents the generation of unwanted spurs inside the system.

Finally, TT&C has a proper DC-DC converter that provides voltages used by all submodules, as well as filter the noise and switching spurs. The supply module converts the unregulated voltage coming from the satellite into a 5V voltage through a DC-DC converter.

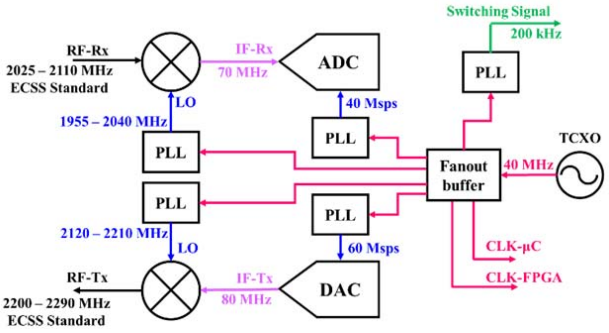

Fig. 5 Frequency plan for the TT&C module

The 5V voltage supplies mostly the analog front-end but it is used also to generate other auxiliary voltages through linear low-dropout regulators. The auxiliary voltages provide the power supply for other components of the TT&C, such as the FPGA and microcontroller. The supply module implements also an over-current protection and an electromagnetic interference filter, enhanced to suppress also the switching spurs and avoid their cross-talk on RF carriers.

B. Sub-Sampling Technique

The pass-band sampling has been chosen in order to simplify both the analog front-end and the digital modem. Typically applied when the SDR approach is used, the pass-band sampling does not constrain the signal to be necessarily modulated/demodulated at base-band. This affects the design of the analog front-end. Since the RF carrier is sampled and digitalized at Intermediate Frequency (IF) frequency, fewer conversion stages will be needed, i.e. fewer components for the analog front-end. Using fewer components has different benefits:

- Fault probability reduction of the components;
- Less effort in the Printed Circuit Board (PCB) design;
- A relaxed image-rejection requirement for the preselector filter;
- Less DC power absorption that saves the satellite energy and at the same time reduces the heat generation (no heat dissipation issues).

However, the pass-band sampling could increase the complexity in the hardware/firmware design of the digital model. A reasonable digitalization of the signal obtaining by

applying the classical Nyquist theorem would have required a 10 oversampling factor in order to reduce effectively the quantization noise. This value of oversampling factor would not be compliant with the 70 MHz IF signal because it would generate a flow of billion of bit (for example at the 8-bit ADC output) to be processed by FPGA. In order to solve this issue, the sub-sampling technique has been applied together with the pass-band sampling. The sub-sampling has had the double benefits to sample the IF signal at a frequency lower than one required by Nyquist theorem and to perform real digital frequency conversion. It has allowed reducing the use of the computation resources because the sub-sampling generates a number of samples smaller than the classic one.

The sub-sampling technique has been used to calculate the right sampling frequency for ADC, i.e. the frequency that does not cause aliasing. Formally, the classic Nyquist theorem is valid only for limited bandwidth signal. The bandwidth of a signal corresponds to the maximum frequency (f_m) over which spectrum energy becomes negligible. In according to Nyquist theorem, the sampling frequency to avoid the aliasing is calculated using (5):

$$f_S \geq 2f_m \tag{5}$$

Equation (5) is valid in general, both for base-band and pass-band signals. However, for pass-band signals, the spectrum energy is mostly centered around the carrier frequency. Defining with B_W the value of maximum frequency (i.e. the bandwidth) of the signal at base-band, applying literally the Nyquist theorem, the sampling frequency for a pass-band signal is calculated using (6):

$$f_S \geq 2(f_C + B_W) \tag{6}$$

where f_C is the carrier frequency.

Looking at (6) under another point of view, the sampler is acquiring not only the samples of the signal but also the sample of its carrier, whose frequency is usually much more greater than the signal bandwidth.

The sub-sampling technique shows that, to prevent aliasing effect, the sampling frequency has to be two times greater than signal bandwidth, without considering the carrier [9]. Since the signal has double energy when it is at pass-band, the formulation of the Nyquist theorem is modified in (7):

$$f_S \geq 2B_W \tag{7}$$

Equation (7) shows that the sampling is still possible even not observing the original formulation of the Nyquist theorem or better still, using a sampling frequency smaller than the maximum frequency of the pass-band signal. However, the condition (7) is not always valid for all values greater than the double of bandwidth because of harmonics. The sampling process generates harmonics at f_S, $2f_S$,…,mf_S where m is an integer [10]. Equation (7) is valid only if the generated harmonics are not overlapped to each other. To avoid harmonic overlapping, the condition to satisfy is given by (8):

$$\frac{2}{m}\left(f_C + \frac{B_W}{2}\right) < f_S < \frac{2}{m-1}\left(f_C - \frac{B_W}{2}\right) \tag{8}$$

or, in equivalent way, by (9):

$$\left[m\frac{f_S}{2}; (m+1)\frac{f_S}{2}\right] \tag{9}$$

Equation (9) highlights that m factor defines specific bands into the spectrum domain, also known as *Nyquist bands*. The width of the Nyquist bands has been designed to be greater than the double of the signal bandwidth, which is in turn calculated in the most conservative case. Looking at the system requirements reported in Table I, the most conservative case is achieved considering the maximum possible bitrate for the QPSK modulation scheme. The signal bandwidth has been calculated using (10):

$$B_W = \frac{R_S(1+\rho)}{2\log_2 M} \tag{10}$$

where ρ is the matching filter roll-off factor and M is the number of symbols on the constellation diagram of the considered modulation scheme. For R_S=1 Mbps and a realistic roll-off factor of 0.5, the bandwidth is 375 kHz.

According to the frequency plan depicted in Fig. 5, choosing a 40 Msps frequency sampling, the Nyquist bands reported in Table II have been obtained following (9).

TABLE II
NYQUIST BANDS FOR 70 MHZ IF AND 40 MSPS SAMPLING FREQUENCY

Band Identification	Frequency range [MHz]	Spectrum type
1st Nyquist band	DC-20 (m=1)	Normal
2nd Nyquist band	20-40 (m=2)	Folded
3rd Nyquist band	40-60 (m=3)	Normal
4th Nyquist band	60-80 (m=4)	Folded

A signal at 70 MHz IF frequency would fall into 3rd Nyquist band if it were sampled by 40 Msps sampling frequency. The sampling system would generate an exact copy of the spectrum signal in the 1st Nyquist band. The signal spectrum is totally within the Nyquist interval because its bandwidth is much smaller than Nyquist band and no aliasing is present. In other words, sampling the signal using frequency smaller than spectrum signal maximum frequency (violating the original formulation of Nyquist theorem), we have not only sampled the signal avoiding aliasing but also indirectly performed a digital frequency conversion. Indeed, the sub-sampling technique can be seen as a digital down-conversion (just as an analog mixer would perform) because the final effect is to have the signal spectrum shifted toward lower frequencies.

In choosing the IF and sampling frequency for sub-sampling design, other factors have to be taken into account, such as the availability of commercial filter and the intrinsic noise performance that arises due to the sampler. The IF frequency choice often depends on a market constraint. Manufacturers design the filters at standard central frequencies following the communication protocol currently available or

basing on the customer requires that have analyzed the spurs into the spectrum and find the best frequency region where is less probable finding in-band spurs. Of course, filter customization is also possible but requires long delivery times.

Regarding the sampling frequency, it has been chosen also taking into account other noise sources generated by the sampling process. Two most relevant noise sources have been investigated: noise due to *aperture jitter* and *noise folding*. The SNR due to jitter depends on the intrinsic aperture jitter (t_{rms}) of the selected COTS ADC and the incoming carrier frequency, according to (11):

$$SNR_j \leq -20\log_{10}(2\pi f_C t_{rms}) \quad (11)$$

For the selected ADC (as described in Section III *D*) t_{rms} is equal to 300 fs rms; therefore, $SNR_j \leq 77.6$ dB. According to (11), increasing the carrier frequency could cause a decrease of the SNR, therefore 70 MHz frequency was the best trade-off between the availability of COTS filters and the degradation of SNR. Instead, noise folding is a phenomenon originated only by the sub-sampling technique. Thermal noise in sampling bandwidth (i.e. the one of the ADC sample-and-hold) is folded into the 1st Nyquist band together with the signal spectrum. The phenomenon depends on the amount of Nyquist bands inside the process, i.e. the m factor. This means that thermal noise is folded m-times into 1st Nyquist band. The m factor depends on sampling frequency according to (8). A simple estimation of the SNR degradation is possible using (12):

$$SNR_f \cong 10\log_{10} m \quad (12)$$

For a 70 MHz carrier, the signal spectrum falls into 3rd Nyquist band, which corresponds a m factor of 3. Therefore, we have obtained a 4.7 dB SNR degradation, which is small enough not to compromise the receiver performance.

C. Definition of the ADC Requirements

In this section, we show that the ADC characteristics have a direct effect on receiver performance. We have selected it both taking into account the sampling frequency previously derived and considering other aspects related to quantization noise, i.e. the SNR of ADC. Being a part of the reception chain, its noise contributes to increasing the total noise of the receiver. Even ADC can be characterized in terms of the noise factor [11]. However, the ADC noise is a combination of the thermal noise and quantization noise, thus noise factor has been calculated taking into account both sources of noise, according to (13).

$$F_{ADC} = 1 + 10^{\left(\frac{10\log_{10}\left(\frac{V_{pp}^2}{2R_{IN}}\right)+30-SNR_{ADC}-10\log_{10}\left(\frac{f_S}{2}\right)}{10}\right)} \quad (13)$$

Equation (13) shows the direct dependency of the noise factor from the SNR of ADC. The SNR is typically provided by ADC datasheet as measured (not theoretical), thus its value represents all noise contributions. Equation (13) is, therefore, the best estimation of the ADC noise performance and it can be easily used to estimate the total noise figure of the receiver (NF_{Rx}) by Friis equation (14):

$$NF_{R_X} = 10\log_{10}\left(F_{chain} + \frac{F_{ADC}-1}{G_{chain}}\right) \quad (14)$$

where F_{chain} and G_{chain} are respectively the noise factor and net gain of the reception chain before ADC.

Equation (14) has been solved numerically evaluating it for different value of the ADC SNR, as shown in Fig. 6. A 0.2 dB degradation of the total noise figure of the receiver has been assumed as caused by the ADC. The curves have been calculated considering the worst-case in terms of the input impedance (R_{IN} = 50 Ω) since commercial ADCs are typically designed to have a higher input impedance. The figure shows that for gain values greater than 70 dB, a 2 dB noise figure is always possible for each ADC SNR considered in the calculation since the gain is at the denominator of (14). Therefore, for high values of the gain, the presence of ADC could be neglectable. However, a higher gain would require many amplification stages. Since one of the final goals of TT&C design is to simplify the hardware design reducing the number of the conversion stages, we have exploited the result depicted in Fig. 6 to search the best trade-off between net gain and ADC SNR requirement.

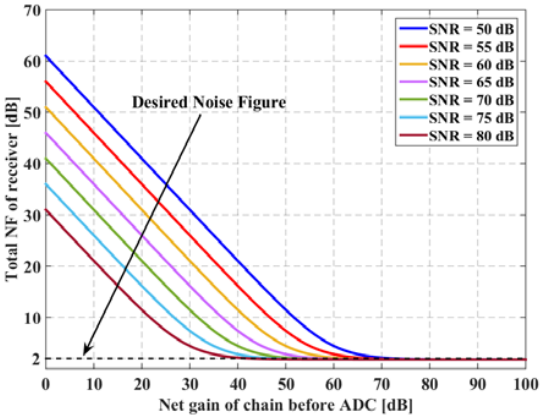

Fig. 6 Total noise figure versus the net gain of the receiver before ADC for different value of ADC SNR (Vpp = 2 V, R_{IN} = 50 Ω, f_S = 40 Msps, $10\log_{10}(F_{chain})$ = 1.8 dB)

The trade-off has been searched taking into account that for each conversion stage (supposing to use a superheterodyne architecture for the receiver) it is possible to set 30-40 dB of net gain before and after mixer not to have oscillation issues. Therefore, the maximum net gain of the receiver should be 60 dB, which corresponds to have an ADC SNR between 60 and 65 dB. This SNR range has been the starting point for the right selection of a COTS ADC.

D. Selection of COTS Components

The selection of COTS components has been based on two aspects:

- Performance requirements;

- Reliability requirements.

Performance requirements have been derived in Section III *C* starting from ADC performance. The receiver has been designed in order to satisfy the following points:

- Superheterodyne architecture with one conversion stage;
- Not more than 60 dB net gain;
- More than 60 dB ADC SNR;
- 2 dB noise figure.

Reliability requirements have been identified taking into account orbital parameters, especially regarding the radiations. The final TT&C has to be a module able to fly and at the same time cheap for the user. Much of the cost of the space modules is caused by electronic parts, which are typically space-qualified. They have a very high level of reliability because they are qualified by long screening processes and test campaigns. It would take even one year to purchase a space-qualified component. The qualification guarantees that the component is able to operate for a certain level of radiation. However, the mission scenario considered in this paper foresees a more relaxed environment. The satellite is at 500 km, where is still protected from the terrestrial magnetic field. A 0.1-1 krad Total Ionizing Dose (TID) range for year is estimated for the satellite that orbits with an orbit angle smaller than 28° and 1-10 krad for higher orbit angles [12]. In addition, components are also protected from the metallic case of the satellite, which reduces further the absorbed TID. Since the TID level is low, to reduce the costs the COTS approach has been exploited. The selected components are not space-qualified. They have been selected anyway with a higher grade of reliability according to ECSS. The selection has been based on the following aspects ordered for priority:

- Heritage availability;
- Any information about the TID;
- Military and automotive qualifications;
- Package and extended temperature range;
- Scientific research regarding technology.

The selection has been done by collecting all available information in order to reduce the risk of using these components. If the information is not available and a component has a critical role inside architecture, a radiation test is foreseen for it. Regarding the package, although the ECSS does not forbid the plastic packages, we have given priority to ceramic packages in order to prevent the outgassing phenomenon and, therefore, unwanted changes in pressure inside the satellite.

The result of the selection is shown in Tables III and IV. Table III reports a summary of the ADC technical performance [13] and Table IV reports the most relevant specifications of the Low-Noise Amplifier (LNA), Mixer, Surface Acoustic Wave (SAW) filter, Adjustable Gain Control (AGC) amplifier, and the transformer [14]-[18].

All selected active components own a heritage, i.e. they have been tested by ionizing radiations. For the VGA, a flight version of the component exists (part number AD8367S) and has been used for the receiver. Regarding the passive components, heritage is, in general, unnecessary, but we have anyway taken into account their reliability looking at the temperature and package.

Table IV reports the main functional parameters typically used to characterize the RF components. For passive parts the absolute value of the gain has been assumed as noise figure; moreover, it is reasonable to suppose that they do not have non-linear behavior, thus a very high value of output third-order intercept (OIP3) has been assumed. The gain parameter has been derived averaging the information collected from datasheets and the S-parameters provided by the manufacturer. Since the information written in datasheets are always reported as graphs, the reading error of the gain curves has been minimized averaging it with the relative S_{21} parameter. This approach has allowed achieving a more realistic value assuming that datasheet data derive from characterization tests on many samples.

TABLE III
PERFORMANCE SPECIFICATIONS FOR ADC

Specification	Value	Unit
Part number	AD9244	-
Heritage	[22]	-
Resolution	14	bit
Sampling frequency	40	Msps
SNR	73.8	dBc
SFDR	84.4	dBc
Differential input voltage range	2	Vp-p
Noise figure	16.8[a]	dB

[a]Calculated using (13) assuming R_{IN}=5kΩ.

TABLE IV
PERFORMANCE SPECIFICATIONS FOR SELECTED COMPONENTS

Part	Type	Gain [dB]	NF [dB]	OIP3 [dBm]	Heritage
ADL5523	LNA	16.5	1	34.2	[19]
HMC422	Mixer	-7.5	8	8	[20]
854653	SAW Filter	-7.5	7.5	111	Not needed
AD8367	AGC	42.5	6.2	34	[21]
T1-1T-X65	1:1 Transformer	-0.6	0.6	111	Not needed

Each parameter has been evaluated at the frequency where the component is logically placed in according to the frequency plan depicted in Fig. 5. For LNA and Mixer, a 2.05 GHz reference frequency (that is within 2025-2110 MHz frequency range of receiver) has been considered since they are placed before the mixer. For SAW filter and the AGC amplifier the 70 MHz reference frequency since they are allocated after the mixer.

IV. Modeling and Results

The modeling has been performed implementing equations for the level budget calculation, starting from the architecture depicted in Fig. 7.

Two cascaded LNAs have been foreseen in order to accomplish the desired net gain and optimize the noise figure. All components shown in Fig. 7 are selected COTS parts, except for the preselector filter that has been realized custom. It has -3 dB in-band attenuation (3 dB noise figure in according to the previous assumption) and more than 30 dB image-frequency rejection. The filter has been designed to

have a 1 dB bandwidth exactly equal to receiver operating frequency defined by requirements, i.e. 85 MHz. SAW filter has a 1 MHz 1 dB bandwidth, which is able to filter QPSK signals at 1 Mbps without letting too much noise enter inside the system which would affect the total noise figure. As well its high selectivity helps to filter any spurs coming from mixer avoiding they get to ADC.

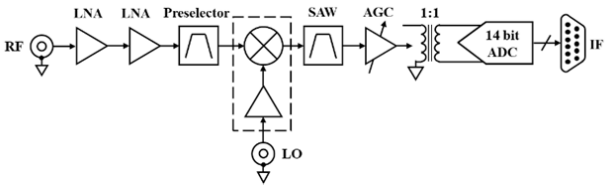

Fig. 7 Receiver high-level architecture

TABLE V
RECEIVER SPREADSHEET DERIVED FROM LEVEL BUDGET EQUATIONS

Index (i)	Part	Type	Gain [dB]	NF [dB]	OIP3 [dBm]	BW [MHz]	TNG [dB]	TNF [dB]	TOIP3 [dBm]	NoiseBW [MHz]	TPSD [dBm]	TSP [dBm]	TP [dBm]	E_b/N_0 [dB]
0	-	-	-	-	-		0.00	0.00	111.00	3600	-78.41	-101.5	-78.39	12.50
1	ADL5523	LNA	16.5	1	34.2	3600.0	16.50	1.00	34.20	3600	-60.91	-84.98	-60.90	11.50
2	ADL5523	LNA	16.5	1	34.2	3600.0	33.00	1.02	34.10	3600	-44.39	-68.48	-44.38	11.48
3	-	Preselector	-3	3	111	85.0	30.00	1.02	31.10	85	-63.66	-71.48	-63.00	11.47
4	HMC422	Mixer	-7.5	8	8	1400.0	22.50	1.04	7.88	85	-71.14	-78.98	-70.48	11.46
5	854653	SAW Filter	-7.5	7.5	111	1.04	15.00	1.13	0.38	1.04	-97.68	-86.48	-86.16	11.37
6	AD8367	AGC	42.5	6.2	34	500.0	57.50	1.45	33.47	1.04	-54.85	-43.98	-43.64	11.04
7	T1-1T-X65	Transformer	-0.6	0.6	111	200.0	56.90	1.45	32.87	1.04	-55.45	-44.58	-44.24	11.04
8	AD9244	ADC	0	16.8	25	750.0	56.90	1.45	24.34	1.04	-55.45	-44.58	-44.24	11.04

The ADC is driven by a transformer that converts the incoming single-ended signal into a differential one required from ADC; as well, it provides a matching impedance. Being passive, it does not have a DC power absorption as an Opamp-type driver would have had, which has allowed decreasing the total DC power consumption of the receiver.

The level budget calculation has been performed for each component at its output calculating the following parameters:

- Linear gain;
- Total noise figure;
- Total OIP3;
- Noise bandwidth;
- Noise power spectral density in the noise bandwidth at that point;
- The power level of the incoming signal starting from the receiver sensitivity (P_{IN}) for the given SNR;
- Total power (noise plus signal power);
- E_b/N_0.

Using an incremental index to identify each component in the reception chain, level budget equations have been rearranged as depicted in Fig. 8. The equations have been written in a recursive form in order to calculate the parameters along all reception chain (not only at the output) and to obtain a spreadsheet of the receiver performance. Results of calculation are reported in Table V for an input carrier at -101.5 dBm that represents the receiver sensitivity at 2 dB noise figure, 10.5 dB E_b/N_0 and 1 Mbps bitrate:

- Receiver noise figure, i.e. TNF(8), is smaller than 2 dB required.
- Receiver net gain, i.e. TNG(8), is about 57 dB, which is close to 60 dB required.
- The SNR, i.e. E_b/N_0(8), is about 11 dB that is even better than the expected one (10.5 dB) at 1 MbpsL.

In conclusion, all specifications are completely fulfilled for a -101.5 dBm receiver sensitivity. The receiver may not be able to capture input signals at a power lower than its sensitivity unless using a channel coding. Having obtained a noise figure lower than the one required has the benefit to give some design margin in order to take into account other impairments not considered in the level budget calculation, such as impedance mismatch, PCB losses, firmware computation losses, etc. The reported analysis has been carried on assuming a perfect 50 Ω matching. Matching has been implemented during the low-level implementation, i.e. schematic.

The maximum signal power that the receiver is able to capture has been evaluated considering the input dynamic range of the AGC amplifier. According to its datasheet [17], the amplifier can vary of 45 dB its power gain. Therefore, the receiver input power range is 45 dB and can accept a -55.5 dBm maximum input power.

The gain control has been customized. Although the amplifier has an internal detector that measures the incoming power and set the output one to a fixed value, such a functionality is not able to measure power levels lower than -34 dBm. The power level at amplifier input is TP(5) according to Table V, i.e. -86.16 dBm. Therefore, the internal detector has been deactivtaded by changing the operational mode of the component (from AGC to VGA), as reported in its datasheet [17], and an external detector has been implemented to read power levels smaller than -34 dBm. The detector has been designed in order to provide the expected output power level according to the obtained spreadsheet.

The power budget has been also estimated calculating for each component of the chain the DC power absorption. Table VI reports the result of this calculation. By adding the absorbed DC powers reported in the fourth column of the table, we have obtained a 1.185 W DC power consumption, which completely fulfills the requirements.

Total Net Gain (TNG)

$$TNG_{dB}(i) = 0\ dB \qquad i = 0$$
$$TNG_{dB}(i) = G_{dB}(i) + TNG_{dB}(i-1) \qquad i > 0$$

Total Noise Figure (TNF)

$$TNF_{dB}(i) = 0\ dB \qquad i = 0$$
$$TNF_{dB}(i) = NF(i) \qquad i = 1$$
$$TNF_{dB}(i) = 10\log_{10}\left(10^{\frac{TNF_{dB}(i-1)}{10}} + \left(\frac{10^{\frac{NF(i)}{10}} - 1}{TNG(i-1)}\right)\right) \qquad i > 1$$

Total OIP3 (TOIP3)

$$TOIP3_{dBm}(i) = 10\log_{10}\left(\frac{1}{TOIP3(i-1) \times G(i)} + \frac{1}{OIP3(i)}\right) \qquad i > 0$$
$$TOIP3_{dBm}(i) = 111\ dBm \qquad i = 0$$

Noise Bandwidth (NoiseBW)

$$NoiseBW(i) = BW(i+1) \qquad i = 0$$
$$NoiseBW(i) = BW(i-1) \quad \text{if } BW(i) \geq BW(i-1) \qquad i > 0$$
$$NoiseBW(i) = BW(i) \quad \text{if } BW(i) < BW(i-1) \qquad i > 0$$

Total Power Spectral Density (TPSD)

$$TPSD_{dBm}(i) = 10\log_{10}(k \times T \times TNG(i) \times TNF(i) \times NoiseBW(i)) + 30 \qquad i \geq 0$$

Total Signal Power (TSP)

$$TSP_{dBm}(i) = P_{IN,dBm} \qquad i = 0$$
$$TSP_{dBm}(i) = G_{dB}(i) + TSP_{dBm}(i-1) \qquad i > 0$$

Total Power (TP)

$$TP_{dBm}(i) = TPSD_{dBm}(i) + TSP(i) \qquad i \geq 0$$

Signal-To-Noise Ratio

$$\left(\frac{E_b}{N_0}\right)_{dB}(i) = TSP_{dBm}(i) - 10\log_{10}(k \times T \times TNG(i) \times TNF(i)) + 30 - 10\log_{10}(R_S) \qquad i \geq 0$$

Fig. 8 Level budget equations rearranged in recursive form

TABLE VI
DC POWER BUDGET CALCULATION

Part	Supply voltage [V]	Absorbed current [mA]	Absorbed DC power [mW]
LNA (x2)	5	60	300 (x2)
Mixer	3	37	111
VGA	5	26	130
ADC	AVDD=5 DRVDD=3	IAVDD=64 IDRVDD=8	320 24

V. CONCLUSION

In this paper, a TT&C subsystem design for LEO small satellites is presented, giving particular attention to the analog receiver. The receiver was designed in different steps: a LBA was performed in order to obtain a 2 dB noise figure requirement; then, high-level architecture and requirements were defined. We have shown that, by implementing the sub-sampling technique, a single-conversion superheterodyne architecture with 57 dB net gain is possible. The chosen architecture has been based on the ADC specifications, whose SNR requirement has been studied. Few components have been needed to implement the architecture. We have shown that it is possible to use COTS parts minimizing the design risk by checking their heritage and by adopting appropriate strategies (like the adoption of ceramic packages, extended temperature ranges, and so on) to prevent the faults and other unwanted phenomena. Finally, the design has been completed calculating the level budget, obtaining excellent performance in terms of noise figure (1.5 dB), E_b/N_0 ratio (11 dB) and power consumption (1.185 W).

ACKNOWLEDGMENT

The Ph.D. student A. Lovascio benefits from a Ph.D. MIUR fellowships for the 2018/2019 academic year, course XXXII, awarded within the framework of the “Programma Operativo Nazionale Ricerca e Innovazione” (PON RI 2014/2020) Axis I “Investments in Human Capital” - Action I.1– “Innovative PhDs with industrial characterization.” Funding FSE-FESR.

REFERENCES

[1] A.Lovascio, A.D’Orazio, V.Centonze, “An Innovative EGSE Approach for Satellite RF system characterization based on Real-Time Monitoring and Space Environment Oriented Analysis,” *2017 IEEE 4th International Workshop on Metrology for Aerospace (MetroAeroSpace)*, Padua, Italy, June 21-23, 2017.

[2] K.M. Davis, "Design of a Small Satellite TT&C Subsystem." *The UNSW Canberra at ADFA Journal of Undergraduate Engineering Research* 7.2 (2015).

[3] R.Omidi, H.Bolandi, B.Ghorbani-Vaghei, S.M.Smaeilzadeh, M.Khayyeri, "An FPGA-based Design Approach for Microsatellites Telemetry Subsystem." *Journal of Telecommunication, Electronic and Computer Engineering (JTEC)* 10.2 (2018): 1-8.

[4] ESA-ESTEC, “Space engineering, Radio frequency and modulation,” ECSS-E-ST-50-05c, Rev.2, Requirements & Standards Division, Noordwijk, The Netherlands, October 4, 2011.

[5] A. Lovascio, D. Cinarelli, G. Mariotti, A. V. Centonze, A. D’Orazio, “An Optimization Method for the Monopole Antenna Placement of a Low-Orbit Small Satellite,” *2018 IEEE 5th International Workshop on Metrology for Aerospace (MetroAeroSpace)*, Rome, Italy, June 20-22, 2018.

[6] W.J. Larson, J.R. Wertz, *Space Mission Analysis and Design*. El Segundo, California: Microcosm Press and Kluwer Academic Publishers, 3rd edition, 2005, ch. 13.

[7] ESA-ESTEC, “Off-the-shelf items utilization in space systems,” ECSS-Q-ST-20-10c, Requirements & Standards Division, Noordwijk, The Netherlands, October 8, 2010.

[8] ESA-ESTEC, “Commercial electric, electronic, and electromechanical (EEE) components,” ECSS-Q-ST-60-13c, Requirements & Standards Division, Noordwijk, The Netherlands, October 21, 2013.

[9] B. Brannon, “Basics of Designing a Digital Radio Receiver (Radio 101),” Analog Devices, Greensboro, NC.

[10] J.R. Gracia Oya, A. Kwan, F.M. Chavero, F.M. Ghannouchi, M. Helaoui, F.M. Lasso, E. Lòpez-Morillo, A.T. Sigado (2012), *Subsampling Receivers with Applications to Software Defined Radio Systems.* In: Zdravko Karakehayov (Ed.), *Data Acquisition Applications,* pp. 165–194, Intech.

[11] J.Karki, "Calculating noise figure and third-order intercept in ADCs." *Analog Applications Journal: Analog and Mixed-Signal Products* (2003).

[12] NASA Technical Memorandum 4322A, “Space Radiation Effects on Electronic Components in Low-Earth-Orbit.” Submitting Organizzation: JSC, lesson 824, February 01, 1999, http://llis.nasa.gov/lesson/824.

[13] AD9244 datasheet (Rev. C), “14-Bit, 40 MSPS/65 MSPS A/D Converter,” Analog Devices.

[14] ADL5523 datasheet (Rev. C), “400 MHz to 4000 MHz Low Noise Amplifier,” Analog Devices.

[15] HMC422 datasheet (v04.0712), “GaAs MMIC MIXER w/ INTEGRATED LO AMPLIFIER, 1.2 - 2.6 GHz,” Analog Devices.

[16] 854653 datasheet (January 31, 2005), “70 MHz SAW Filter,” SAWTEK (a TriQuint company).

[17] AD8367 datasheet (Rev. A), “500 MHz, Linear-in-dB VGA with AGC Detector,” Analog Devices.

[18] T1-1T-X65 datasheet (Rev. B), “RF Transformer, 50 Ω, 0.08 to 200 MHz,” Mini-Circuit.

[19] A.S.Y.M.H. Habaebi, S.N. Ibrahim, N.F. Hasbullah, “Gain Investigation for commercial GaAs and SiGe HBT LNA’s under Electron Irradiation,” *2016 IEEE Student Conference on Research and Development (SCOReD)*, Kuala Lumpur, Malaysia, December 13-14, 2016.

[20] M.V. O’Bryan, K.A. LaBel, J.A. Pellish, J. Lauenstein, D. Chen, C.J. Marshall, T.R. Oldham, H.S. Kim, A.M. Phan, M.D. Berg, M.J. Campola, A.B. Sanders, P.W. Marshall, M.A. Xapsos, D.F. Heidel, K.P. Rodbell, J.W. Swonger, D. Alexander, M. Gauthier, B. Gauthier, “Recent Single Event Effects Compendium of Candidate Electronics for NASA Space Systems,” *2011 IEEE Radiation Effects Data Workshop*, Las Vegas, NV, USA, July 25-29, 2011.

[21] AD8367S flight datasheet (Rev .C), “500 MHz, Variable Gain Amplifier with Automatic Gain Control Detector,”

[22] G. R. Allen, “Compendium of Test Results of Single Event Effects Conducted by the Jet Propulsion Laboratory,” *2008 IEEE Radiation Effects Data Workshop*, Tucson, AZ, USA, July 14-18, 2008.